Nitrogen Oxide Formation in the Electric Arc Furnace – Measurement and Modeling

The final publication is available at Springer via http://dx.doi.org/10.1007/s11663-011-9564-8

NO_x formation in the electric arc furnace – measurement and modelling

Dr.-Ing. Thomas Echterhof, Prof. Dr.-Ing. Herbert Pfeifer

RWTH Aachen University, Dept. for Industrial Furnaces and Heat Engineering,

Kopernikusstr. 10, 52074 Aachen, Germany

Abstract

In this paper the results of pilot EAF trials and model calculations regarding the formation of NO_x in an electric arc furnace are presented. The results of these investigations confirm that the conditions within the electric arc furnace are favourable for the formation of NO_x. During pilot furnace trials a notable influence of the electric parameters on the NO_x formation could not be established. The importance of the influence of the furnace atmosphere, especially the O_2 and CO content, could be clearly ascertained.

Thermodynamic equilibrium calculations concerning the furnace atmosphere were conducted during the course of the investigations. The results clearly show that the chemical reaction kinetics have a considerable influence on the NO_x concentrations measured in the off-gas of electric arc furnaces. Therefore, in addition to the equilibrium calculations a reactor network model of the EAF was subsequently developed. Using this model it was possible to reproduce phenomena such as the NO_x peak at arc ignition as well as to calculate NO_x concentrations, which match measurement data within an order of magnitude.

Keywords: NO_x formation, pilot EAF, thermodynamic calculation, reactor network model

I. INTRODUCTION

The electric arc furnace (EAF) is an important production unit with regard to the worldwide steel production. 30.6 % of the world's crude steel production of 1.3 billion tons was produced in EAF's in 2008. Apart from productivity and operational efficiency, it is also important for the operator of an EAF to ensure that the emission of greenhouse gases such as CO_2 or nitrogen oxides stays within the limits of environmental regulation requirements.

Nitrogen oxides (NO_x) are the second most important air pollutant after CO_2 during steel production. NO_x emissions at an EAF depend on operational modes (use of gas burners, oxygen injection etc.) as well as operating parameters such as arc length, arc ignitions etc., which are usually fast changing due to the batch operation of the furnace. The EAF has conditions theoretically favourable for the formation of NO_x. These are N_2, O_2 and CO_2 containing furnace atmospheres, high gas temperatures of up to 2,000 K, electric arcs with currents of up to 100 kA and an arc plasma with temperatures of up to 8,000 to 10,000 K. Nevertheless there is almost no research concerning NO_x emissions at an EAF published in Europe and only a small number of publications from North America and Japan [1-4] are available.

Previous measurements of the NO_x emissions at industrial EAFs[5,6] showed that to fully understand the influence of the different mechanisms of NO_x formation on the emissions of the EAF additional investigations at a pilot arc furnace were needed. This paper presents a summary of the results of such measurements carried out under the controlled conditions of a pilot furnace. In addition the measurements were accompanied by comparative model calculations based on thermodynamic equilibrium calculations and furthermore a reactor network model to take chemical reaction kinetics into account was developed. The results of the model calculations are also presented and discussed in this paper and compared to the measurement data.

II. NO_X FORMATION

'Nitrogen oxides' is the generic term for a group of air pollutants including nitric oxide NO, nitrogen dioxide NO_2 and nitrous oxide N_2O. Even though all three components usually occur concurrently, NO is generally the main constituent of NO_x, accounting for more than 90 %.

The three main formation mechanisms for NO_x are the thermal NO_x mechanism, the fuel NO_x mechanism and the prompt NO_x mechanism. As far as high temperature processes are concerned, the main source for NO_x is typically thermal NO_x, which is based on the oxidation

of atmospheric nitrogen at high temperatures. Since this reaction mechanism is very temperature dependent, it is very relevant for the NO_x formation in the electric arc. The mechanism for the formation of thermal NO_x, also known as the extended Zeldovich mechanism[7,8], is given by the equations [1] to [3].

$$N + O_2 \rightarrow NO + O \quad [1]$$

$$O + O^2 \leftarrow \rightarrow NO + O \quad [2]$$

$$N + OH \leftrightarrow NO + H \quad [3]$$

Fuel NO_x is formed by the oxidation of fuel bound nitrogen. This fuel bound nitrogen occurs in fossil fuels such as coal and heavy fuel oil or coke oven gas. Burning these fuels leads to the oxidation of a substantial fraction of the fuel bound nitrogen to NO according to eq. [4].

$$2[N]_{fuel} + O_2 \rightarrow 2\,NO \quad [4]$$

The formation of prompt NO_x is more complex and controlled by the formation of CH radicals. The CH radicals react with nitrogen to HCN and the HCN then reacts in several subsequent steps to NO_x according to equation [5]. The prompt NO_x formation, because of its CH dependency, is highly dependent on local fuel concentration[8]. In the EAF it is usually less relevant than thermal NO_x.

$$CH + N_2 \rightarrow HCN + N \ldots \overset{NO}{N_2} \quad [5]$$

III. PILOT FURNACE TRIALS

The measurements described within this paper were conducted in a gas tight pilot EAF, as shown in Figure 1. The furnace has a capacity of approximately 150 kg of melt and was used in DC-mode with one electrode and a maximum electrical power of 300 kW. The furnace can be sealed off, so that no leak air intake is possible. It is also equipped with a gas supply system, based on a set of mass flow controllers and a ring line in the furnace, so that defined premixed gas atmospheres and volume flow rates can be set within the furnace freeboard. During the trials at the pilot furnace, the composition and temperature of the off-gas as well as operating parameters of the mass flow controllers and of the furnace, such as power, arc current, arc length etc., were recorded continuously. Nitrogen oxides were measured by a chemiluminescence detector (CLD) as NO_x, the sum of NO and NO_2.

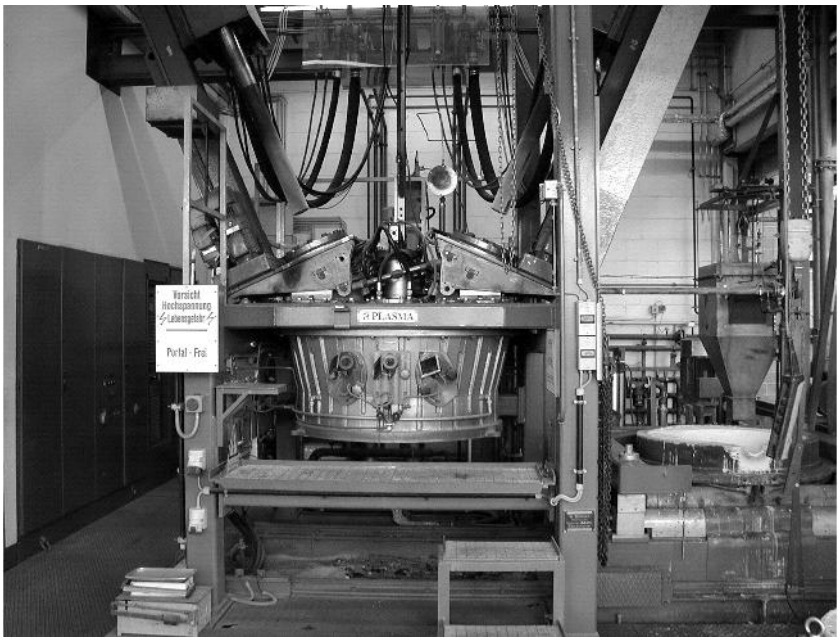

Figure 1: Pilot electric arc furnace

The aim of the measurements in the pilot EAF was to investigate the formation of NO_x in dependency of varying process parameters and furnace atmospheres. Therefore, in a first group of trials the arc was ignited for short time periods in preset atmospheres in a cold furnace. During these trials there was no significant amount of steel melt or slag formed. This is comparable to the arc ignition in an industrial furnace after charging. The furnace atmospheres were preset by purging the furnace with a constant gas volume flow with a given composition, which was controlled by a group of mass flow controllers (cf. Figure 2). In this way, specific N_2, O_2, CO etc. concentrations of the furnace atmosphere prior to arc ignition could be set. Following the arc ignition, the arc length and current were varied.

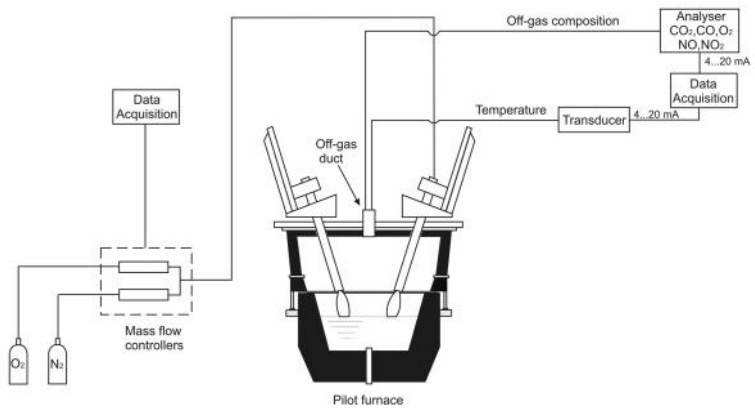

Figure 2: Schematic of the gas tight pilot EAF with gas supply system and off-gas analyser

In Table I the parameters and variation thereof during these first trials are shown. As far as the furnace atmosphere is concerned, mainly the relation of O_2 to N_2 concentration was varied, since this was expected to have the biggest influence on NO_x formation.

Table I: First group of trials at pilot EAF

Trial	Description	Power
Trial 1.1	Arc ignition in air	100 to 150 kW
Trial 1.2	Arc ignition in air	120 kW
Trial 1.3	Arc ignition in 17.8 % O_2 / 82.2 % N_2	120 kW
Trial 1.4	Arc ignition in 9.9 % O_2 / 90.1 % N_2	120 kW
Trial 1.5	Arc ignition in 1 % O_2 / 99 % N_2, Addition of 5 % CO_2	200 to 300 kW
Trial 1.6	Arc ignition in 1.5 % O_2 / 98.5 % N_2, Addition of 5 % CO_2	200 kW
Trial 1.7	Arc ignition in air, Addition of N_2	150 kW
Trial 1.8	Arc ignition in 4.5 % CO_2 / 95.5 % N_2, Increase of CO_2 addition from 5 % to 10 %	100 to 200 kW
Trial 1.9	Arc ignition in 2 % CO_2 / 98 % N_2	75 to 150 kW
Trial 1.10	Arc ignition in air	100 to 200 kW

Table II: Process parameter variation in second group of trials at pilot EAF

Trial	Gas composition (balance N_2) [%]			Volume flow rate [l/min]
	O_2	CO	CO_2	
Trial 2.1	0 to 21	0 to 12	0	70
Trial 2.2	7.5	0	0	200
Trial 2.3	0 to 19.7	0	0	60 to 225
Trial 2.4	12.25 to 15.75	0	0 to 1.5	160 to 200
Trial 2.5	0 to 15	0	0	100
Trial 2.6	17 to 20	5 to 20	0	100

In a second group of trials the furnace was first operated until it was in a thermally stable ‘hot’ state with a liquid melt pool inside. The melt mainly consisted of liquid steel. Only a small amount of slag was present, formed by the oxidation of iron. No slag formers were added and the slag was not foamed, since this would have led to high amounts of CO in the

furnace atmosphere, thereby reducing any NO_x formed in the arc. Only after reaching the thermally stable state the actual trials were conducted. During these trials arc length and current as well as the composition of the gas fed into the furnace and its volume flow rate were varied. Table II gives an overview of the conducted trials and the varied parameters.

IV. RESULTS OF TRIALS

A first unexpected result of the trials was the unverifiable influence of the electric parameters such as power, arc current and length within the operational limits of the pilot EAF on the NO_x formation. As can be seen in Figure 3, any influence of the electric operation parameters of the EAF is covered by other more dominant effects such as in this case the influence of an increasing CO concentration. Therefore within the limits of realizable trial conditions at the pilot EAF no correlations between electric parameters and NO_x formation could be established. Therefore when considering only the electric parameters of the arc, the amount of generated NO_x can be assumed to be constant, as long as the arc is burning in the furnace.

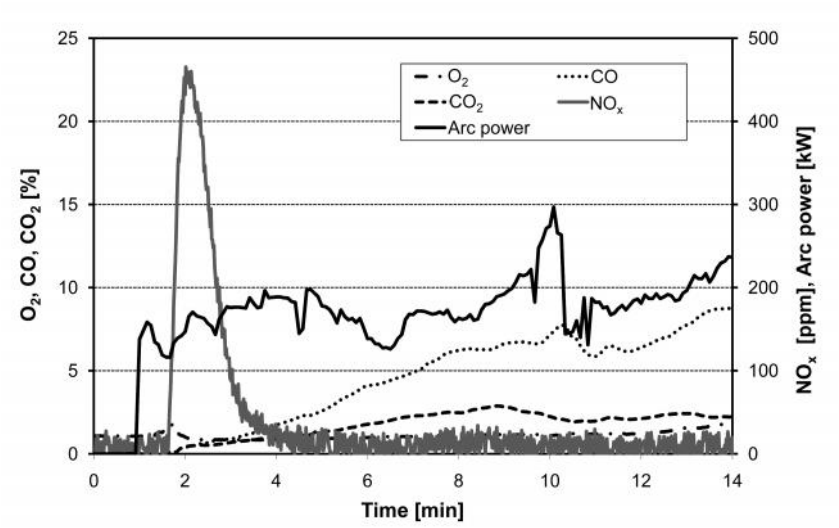

Figure 3: Exemplary trial with variation of the arc power

By comparison, the formation of NO_x is much more dependent on the furnace atmosphere in which the arc is ignited or in which it burns. Figures 4 and 5 show the effect of oxygen depletion of the atmosphere on NO_x formation at arc ignition. A reduction of the oxygen concentration in the furnace from 17.8 % to 9.9 % leads to a decrease of the measured NO_x content in the furnace off-gas of 50 % from about 2,000 to 1,000 ppm.

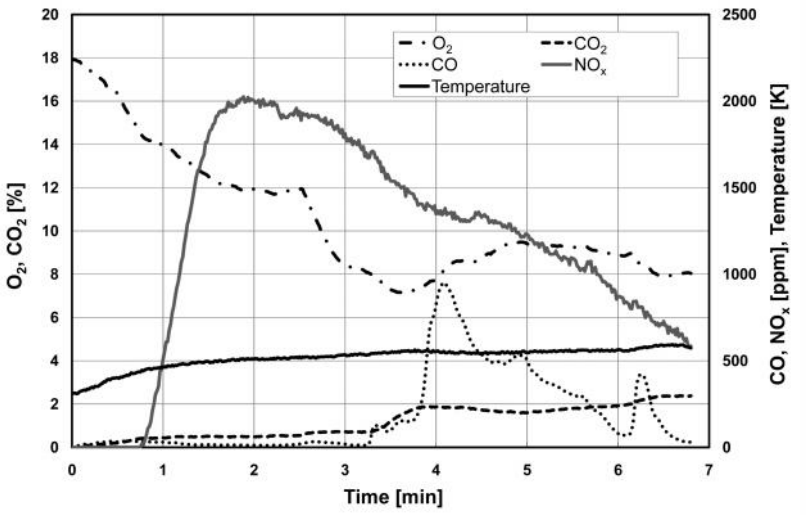

Figure 4: Arc ignition in 17.8 % O_2 and 82.2 % N_2 atmosphere

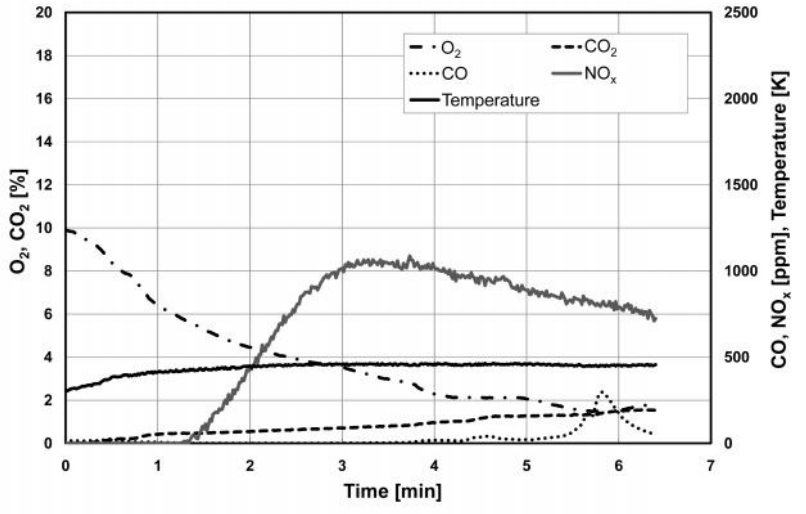

Figure 5: Arc ignition in 9.9 % O_2 and 90.1 % N_2 atmosphere

The measurement results for an arc ignition in an oxygen free CO containing atmosphere as well as for an arc ignition in an oxygen containing atmosphere are shown in Figure 6. The typical NO_x peak at arc ignition, also known from measurements in industry, is only present for the ignition in oxygen containing gas.

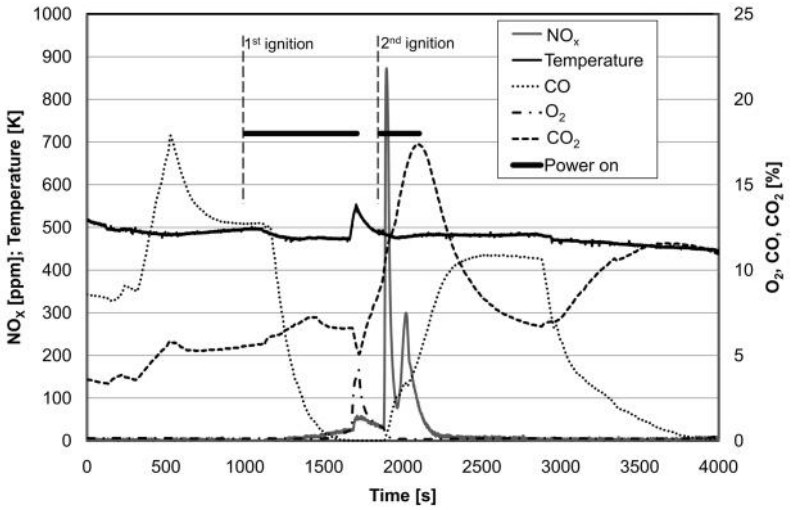

Figure 6: Arc ignition in CO containing O_2 free atmosphere (first ignition) and in oxygen containing atmosphere (second ignition)

Figure 7 shows exemplary operational and measurement data of one of the 'hot' trials of the second group (Trial 2.4, cf. Table II). During this trial the oxygen content of the gas mixture fed into the furnace as well as its volume flow rate were varied. The flow rate was changed in the range of 60 to 225 l/min and the oxygen concentration of the gas was varied between 0 % and 19.7 %. As can be seen from the results there is an indirect influence of the volume flow rate on the NO_x concentration in the off-gas via the retention of the gas in the furnace. Flow rates below 150 l/min lead to an increase in the CO content in the furnace, due to the accumulation of CO from the oxidation of the electrode. This increase in CO content leads to low O_2 and NO_x concentrations in the off-gas. At volume flow rates above 150 l/min only small amounts of CO and NO_x concentrations of up to 6,000 ppm were measured.

Trial 2.4 was also evaluated with regard to the dependency of NO_x concentration on the O_2 and CO content of the off-gas. A correlation between CO_2 concentration and NO_x content could not be found, even though the thermodynamic equilibrium calculations, described later in this paper, indicate such an influence.

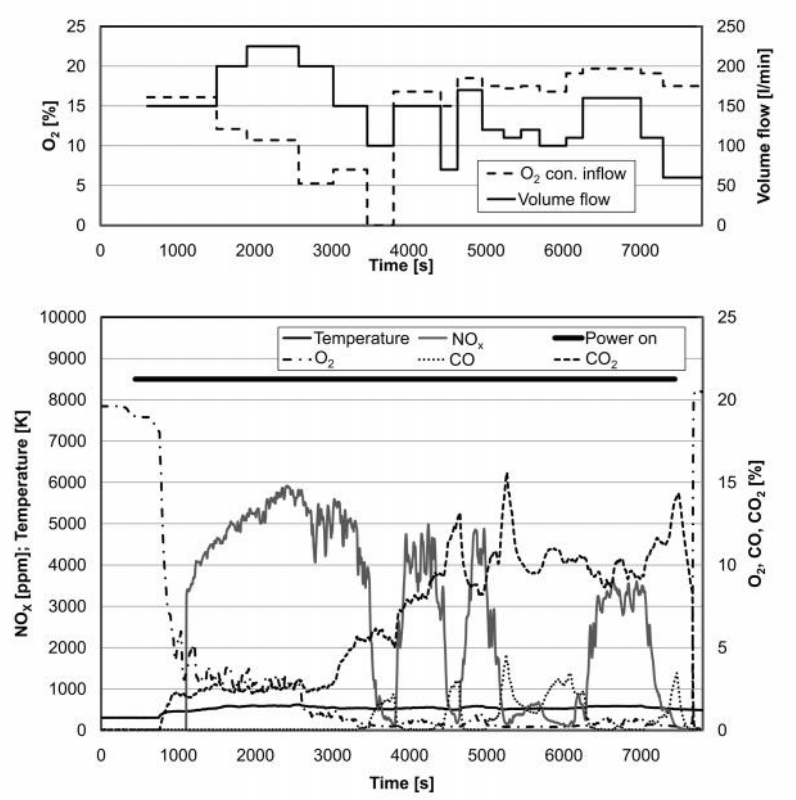

Figure 7: Trial 2.4 with varying O_2-N_2 ratio and volume flow rate

Figure 8 shows the correlation between the NO_x and O_2 concentration in the off-gas of trial 2.4. In Figure 8 it is clearly recognisable that with a decreasing O_2 concentration approaching 0 % a steep decline of the NO_x content also approaching 0 ppm occurs. The result of the nonlinear regression analysis, shown by the logarithmic graph in Figure 8, leads to the conclusion that for the given trial at oxygen concentrations below 0.18 % there is not enough oxygen in the furnace atmosphere to form measureable amounts of NO_x.

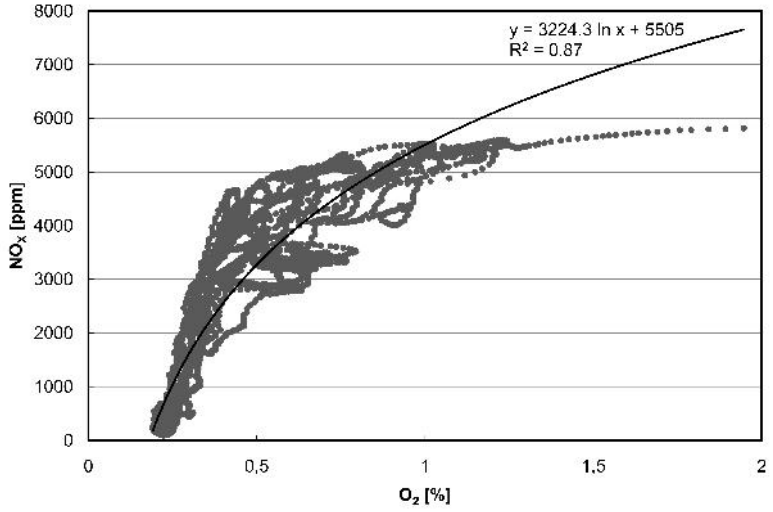

Figure 8: NO_x concentration as a function of the O_2 concentration in the off-gas of trial 2.4

The correlation between CO and NO_x content of the off-gas is shown in Figure 9. There is a strong correlation between decreasing NO_x concentrations and increasing CO concentrations. This is partly due to the related correlation between rising CO and decreasing O_2 concentration, but is also due to the reducing capability of CO on NO_x. According to the exponential function of the regression analysis, at CO concentrations of over 3 % the NO_x level in the off-gas should be below 150 ppm.

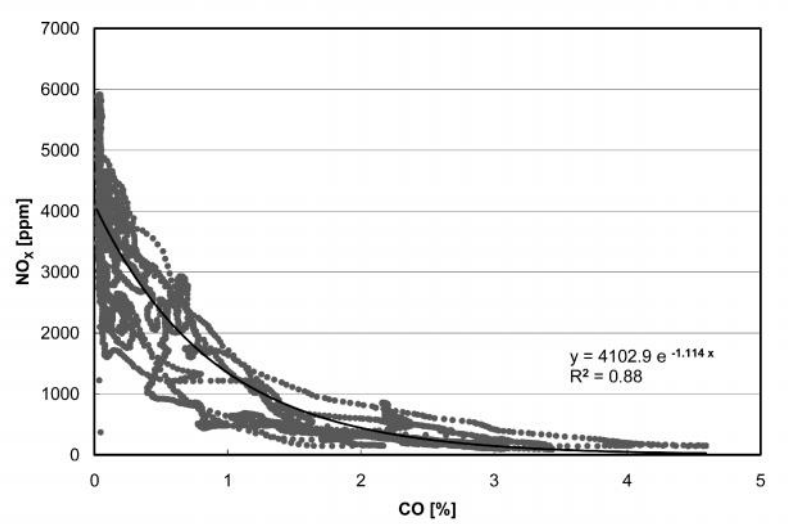

Figure 9: NO_x concentration as a function of the CO concentration in the off-gas of trial 2.4

To further investigate the correlation of the NO_x concentration and the O_2 and CO content in the off-gas, the aggregated measurement data of the second group of trials was used. In Figure 10 the NO_x content of the off-gas is presented in a 3D diagram in relation to the CO and the O_2 concentration. Once again the diagram demonstrates that the highest NO_x concentrations were measured at oxygen concentrations of 2 to 13 % and in absence of CO. The lowest NO_x concentrations on the other hand were measured between 0 and 1 % O_2 with the simultaneous presence of CO in the off-gas.

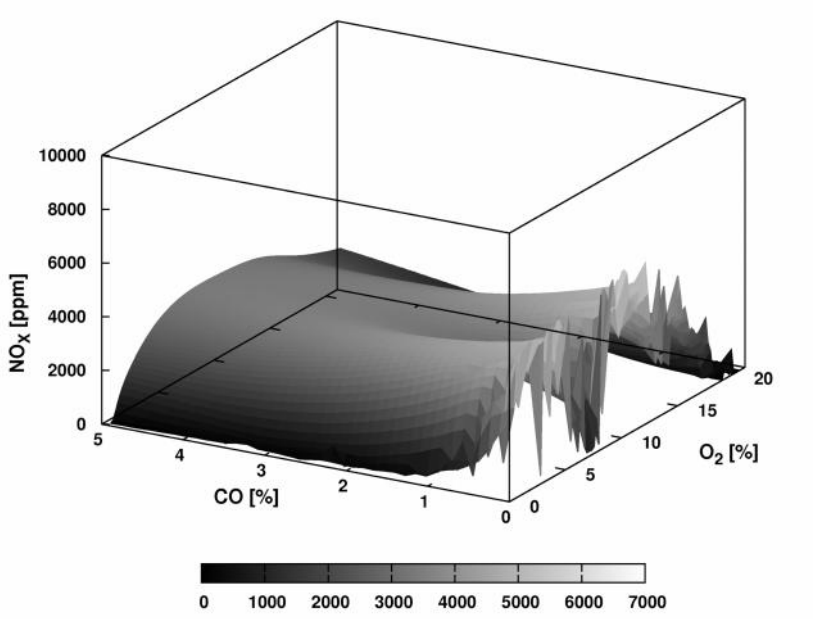

Figure 10: NO_x concentration as a function of the CO and O_2 concentration in the off-gas

V. THERMODYNAMIC EQUILIBRIUM CALCULATIONS

The thermodynamic calculations as well as the subsequent chemical reaction kinetics calculations are based on the thermochemical data of the GRI-MECH 3.0 database[9]. The calculations were carried out using the Cantera software package[10].

The thermodynamic calculations were used to determine the equilibrium concentration of the individual gas species for a given composition and temperature of the gas phase in the EAF. The furnace atmosphere composition at a state of thermodynamic equilibrium was determined by minimizing the Gibbs free energy ΔG for the given composition and temperature. Since NO_2 and N_2O concentrations for all thermodynamic calculations were below 1 ppm, the results for these two species are omitted from the figures 11-14 and only the NO concentration is shown.

First the thermodynamic equilibrium compositions for several O_2-N_2 mixtures were calculated. The oxygen content in the mixture was set to 21, 10 and 5 % and the temperature was varied between 1,000 and 3,500 K. Figure 11 shows the results of these calculations. Up to temperatures of 1,700 K (1,427°C) and even for an oxygen concentration of up to 21 % the NO_x content of the mixture in thermodynamic equilibrium is quite low (< 30 ppm). At higher temperature (> 2,000 K) increasing amounts of monoatomic oxygen are stable. This contributes according to the Zeldovich mechanism (cf. eq. [1]) to the formation of nitrogen oxides and leads to the highest amounts of NO being calculated for temperatures above 3,000 K.

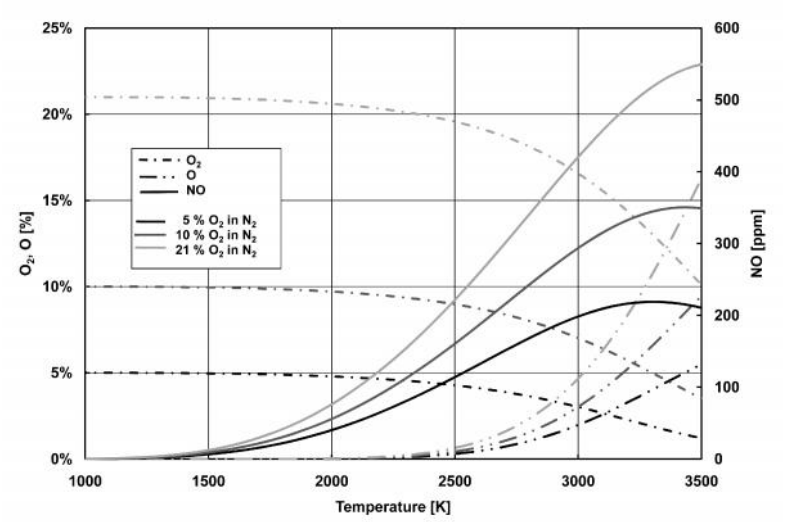

Figure 11: Thermodynamic equilibrium composition of O_2-N_2 gas mixtures

In Figures 12 to 14 the influence of reducing gas species such as CO, H_2 and, because of its dissociation at high temperatures, also CO_2 on the NO concentration in equilibrium is depicted. All gas mixtures are based on 10 % O_2 and with N_2 making up the balance. The figures show that in the presence of reducing gas species an even lower amount of NO results in the equilibrated mixtures. For a CO-O_2-N_2 mixture in the temperature range of 1,000 to 3,500 K and with CO concentrations of 5, 25 and 50 % the calculated gas composition of the equilibrated mixture is shown in Figure 12. For 5 % CO in the initial mixture a NO concentration in equilibrium of 17 ppm is calculated at 1,700 K. Higher CO concentrations lead to NO concentrations of under 0.01 ppm at this temperature.

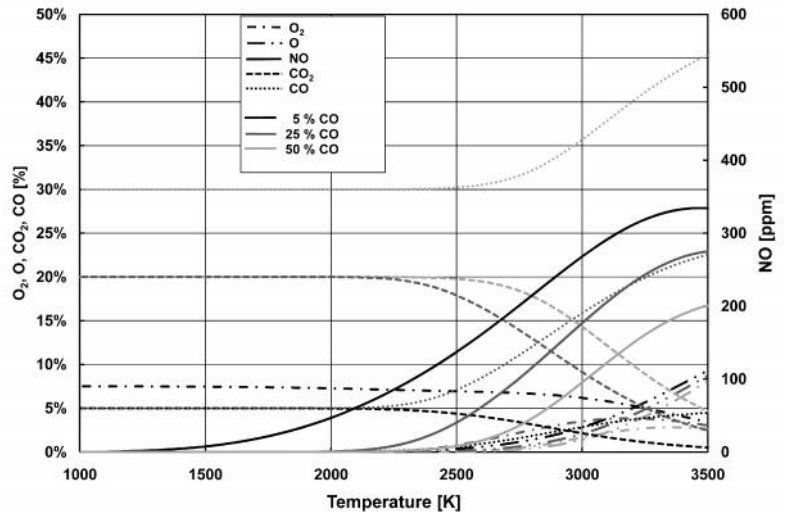

Figure 12: Thermodynamic equilibrium composition of CO-O_2-N_2 gas mixtures (with 10 % O_2 and N_2 balance)

The thermodynamic equilibrium compositions for several H_2-O_2-N_2 mixtures are shown in Figure 13. The initial hydrogen content was varied between 5 and 15 %. For 5 % hydrogen in the initial mixture the NO concentration at 1700 K was calculated to be 13 ppm. Contrary to this, the CO_2 content in a CO_2-O_2-N_2 mixture has only a small influence on the NO concentration at temperatures up to 1,700 K (Figure 14). A NO decreasing effect of CO_2 is noticeable for considerably higher temperatures (> 2,000 K).

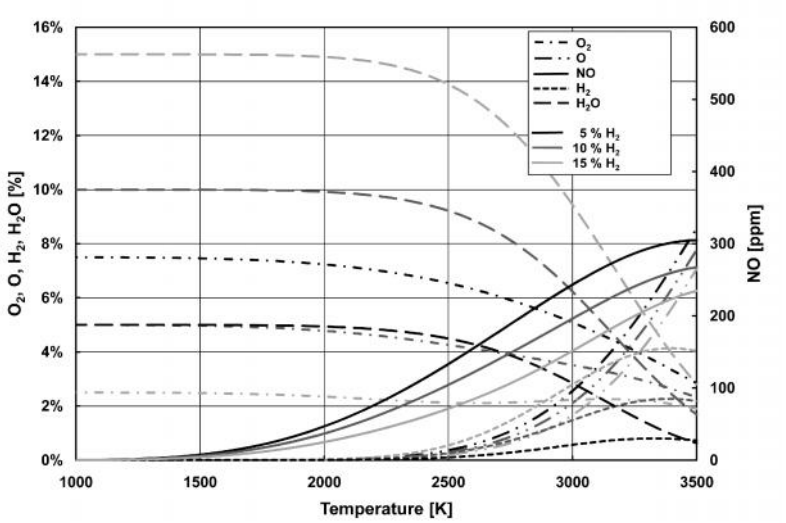

Figure 13: Thermodynamic equilibrium composition of H_2-O_2-N_2 gas mixtures (with 10 % O_2 and N_2 balance)

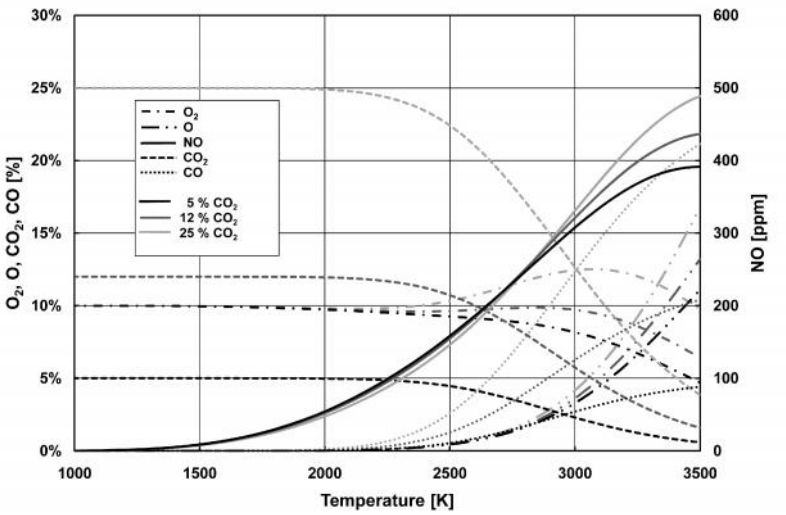

Figure 14: Thermodynamic equilibrium composition of CO_2-O_2-N_2 gas mixtures (with 10 % O_2 and N_2 balance)

The thermodynamic calculation results show that in thermodynamic equilibrium at temperatures of up to 1,700 K only small amounts of NO (< 30 ppm) are stable. In the

presence of reducing gas species such as CO or H_2 the equilibrium concentration of NO is even lower.

A comparison of these thermodynamic calculation results with the measurements of the pilot EAF trials and with industrial measurements shows, that the amount of NO_x measured in the furnace off-gas is generally higher than predicted by thermodynamic calculations. Thus the off-gas of an EAF usually is not in thermodynamic equilibrium, which can be attributed to high off-gas volume flow rates and short retention times of the gas in the furnace freeboard. This leads to the freezing of high NO_x concentrations in the gas mixture. The NO_x peaks often seen in off-gas measurement data such as Figure 15 correlate with high oxygen concentrations in the off-gas and low off-gas temperatures at the furnace exit and therefore can be attributed to thermally inhibited reaction kinetics. These conditions are typical for the arc ignition phase after opening and charging of the furnace.

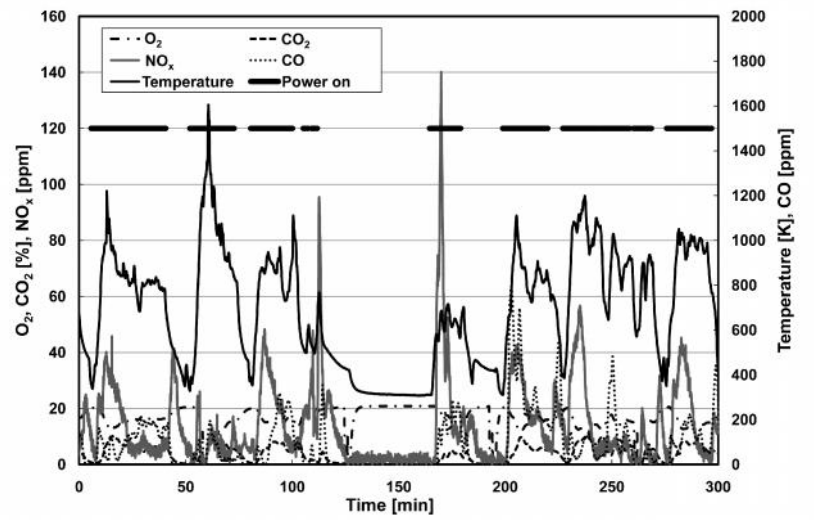

Figure 15: Measured off-gas composition and temperature for an exemplary industrial heat after post-combustion

VI. CHEMICAL KINETICS CALCULATIONS

Based on the results of the thermodynamic equilibrium calculations, the next logical step was to investigate the influence of reaction kinetics on the NO_x formation. Therefore the EAF was subsequently modelled by idealising it as a continuous ideally stirred tank reactor (CSTR) network. Once more the Cantera software package was used. A schematic of the resulting reactor network model is shown in Figure 16. This simplified model is mainly based on two CSTRs. Reactor 1 represents the furnace freeboard and Reactor 2 represents the arc plasma volume. The reactors are characterized by volume, temperature, pressure, and the initial composition of the gas inside each volume. As shown in Figure 16, Reactor 1 is fed from two

reservoirs, Res 1 and Res 2, and the mass flow from these reservoirs into the reactor is in each case controlled by a mass flow controller (MFC). From Res 1 air representing leak air is fed into the furnace. From Res 2 a defined mass flow of carbon can be supplied to Reactor 1. The gas mixture generated in Reactor 1 can stream out via Valve 2 into a collecting reservoir (Res 3) with almost no pressure difference between Reactor 1 and Res 3. The electric arc inside the furnace is modelled using Reactor 2. A fraction of the gas inside Reactor 1 is circulated through the arc plasma Reactor 2 by MFC 3.

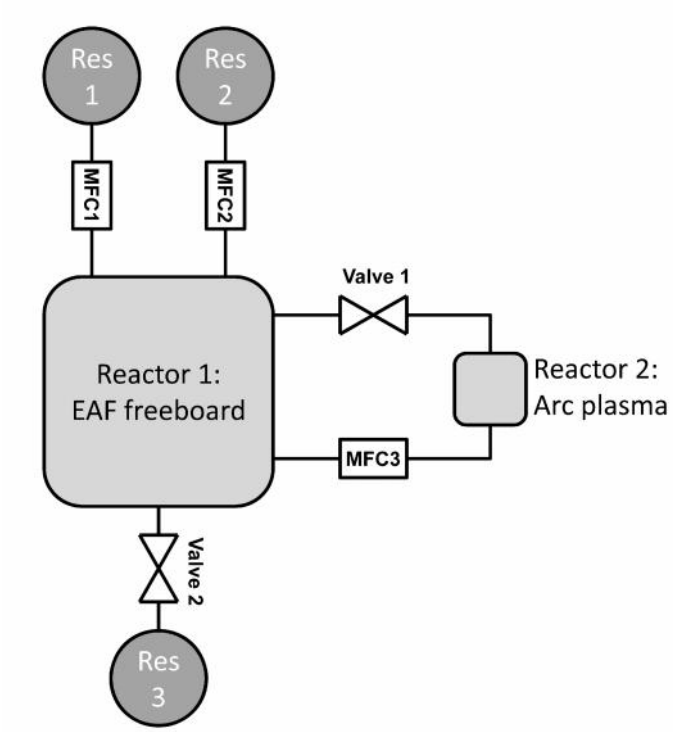

Figure 16: Schematic of the EAF reactor network model

Table III: Initial set of parameters for reactor network model

	Volume	Temperature	Pressure	Gas composition	Mass flow rate
res 1		300 K		air (79 % N_2, 21 % O_2)	
res 2	-	300 K		C	
res 3		300 K	1 bar	air (79 % N_2, 21 % O_2)	-
reactor 1	106.25 m^3	1,973 K		air (79 % N_2, 21 % O_2)	
reactor 2	0.00192 m^3	9,000 K		air (79 % N_2, 21 % O_2)	
MFC 1					3.52 kg/s
MFC 2			-		0 kg/s
MFC 3					0.324 kg/s

An initial set of parameters for this model is given in Table III. This set of parameters is based on those of an industrial electric arc furnace. In addition to the off-gas measurements at the pilot furnace measurements were also conducted at this specific industrial EAF. The results are shown in Figure 15. The EAF is a 140 t AC furnace with an installed transformer power of 105 MVA producing stainless and carbon/tool steel grades. The furnace is equipped with a lance manipulator for oxygen, coal and dust injection. During carbon steel heats, oxygen and carbon are injected to foam the slag and during stainless steel heats oxygen is injected to decarburize the melt.

The modelled EAFs freeboard volume is based on engineering drawings of the industrial EAF. The temperature of the furnace atmosphere is set to a constant value. Because of the lack of temperature measurement data inside the furnace, the atmosphere temperature was varied during the calculations in the range from 1,773 to 2,173 K (1,500 to 1,900°C), based on off-gas temperature measurements conducted at the elbow of various industrial EAFs. The leak air volume flow was derived from operational measurements and mass balances and was varied in a range of 2 to 10 kg/s in order to investigate its influence on NO_x formation. The carbon mass flow into the reactor was obtained based on mass balances carried out for the industrial EAF by using off-gas volume flow measurements and off-gas analysis data. It was varied between 0 and 2 kg/s to investigate the influence of electrode burn-off, carbon injection and decarburization on the NO_x content of the furnace atmosphere. The volume of the arc plasma reactor as well as the mass flow into it was calculated using operational data and a channel arc model for electric arcs[11]. The values were varied with respect to the calculated base value ($V_{reactor\ 2}$: 0.001 to 0.003 m³; mass flow MFC3: 0.1 to 0.6 kg/s) to investigate the influence of arc length and arc power. The temperature of the arc plasma reactor was varied in the range of 7,000 to 11,000 K.

The resulting composition of the gas mixture in the EAF freeboard (Reactor 1) as a function of simulated time is shown in Figure 17 for the initial set of parameters. Within seconds a steady NO concentration of over 10,000 ppm is reached in this simulation. However this set of parameters would only describe the very first seconds of a heat, the arc ignition in a cold furnace. During the transient process in the EAF, shortly after arc ignition, the electrode burn-off begins and as a result carbon is added to the furnace atmosphere. Assuming an electrode consumption of 2-3 kg/t_{steel} and an average heat duration of one hour, the carbon addition for the modelled 140 t EAF from the electrode burn-off is about 0.08-0.12 kg/s.

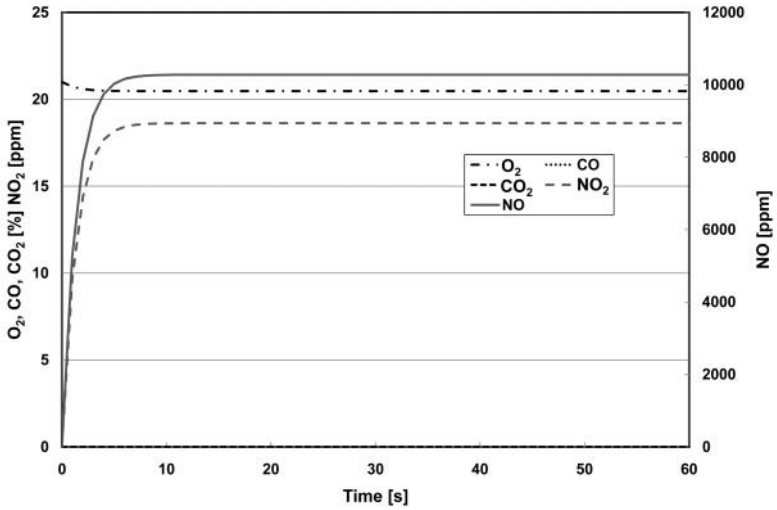

Figure 17: Gas composition in the EAF freeboard reactor as a function of time for the initial set of parameters

As soon as not only air, but also carbon is fed into the EAF freeboard, NO peaks occur in the temporal course of the simulation. This corresponds to observations during measurements at the pilot furnace and in industry, where such peaks are typical. Sources for carbon in the EAF are oxidation of the graphite electrodes as well as slag foaming or decarburization. Figure 18 depicts the gas composition in Reactor 1 with respect to the simulated time for the case of a 0.5 kg/s carbon addition. The 0.5 kg/s represents an average value during a heat for the carbon mass flow during stainless steel production at the investigated EAF.

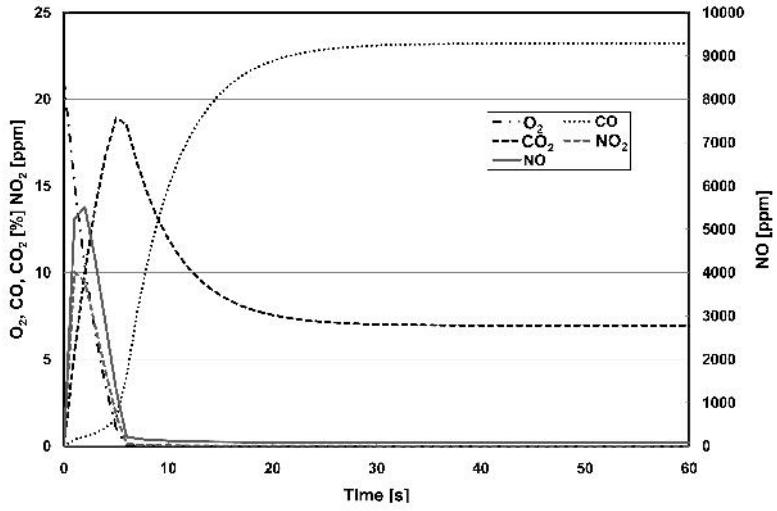

Figure 18: Gas composition in the EAF freeboard reactor as a function of time for 0.5 kg/s carbon addition

To investigate the influence of the different model parameters on the amount of formed NO_x, the parameters were varied with respect to the initial set. Since NO and NO_2 show a very

similar progression (cf. Figure 17 and 18), only NO concentrations are presented in Figure 19 to 21. Figure 19 shows the influence of the EAF freeboard reactor parameters on the maximum NO content in the EAF (NO_{max}). While the decreasing NO_{max} content with increasing air mass flow can easily be explained by dilution effects, the variation of the EAF freeboard temperature leads to a minimum of the formed NO_{max} at temperatures of 1,973 to 2,073 K (1,700 to 1,800°C). Therefore it can be concluded that at 1,973 K (1,700°C) there is no negative effect from an increased nitrogen inflow, as supplied by the higher amounts of leak air, but only a dilution effect decreasing the NO_{max} concentration in the furnace atmosphere. The observed concentration minimum while varying the temperature may be due to a shift in the equilibrium between NO_x reducing and NO_x forming reactions in the furnace atmosphere. For temperatures up to about 1,973 K (1,700°C), the NO_x reducing reactions are dominant and the increase in temperature leads to an increased NO_x reduction. At the observed NO_{max} minimum, the equilibrium shifts in favour of the NO_x forming reactions and with increasing temperature disproportionally more NO_x is formed in the EAF freeboard than is reduced. So an increase of the temperature inside the furnace freeboard, for example by oxygen injection for post combustion, will lead to increased NO_x concentrations.

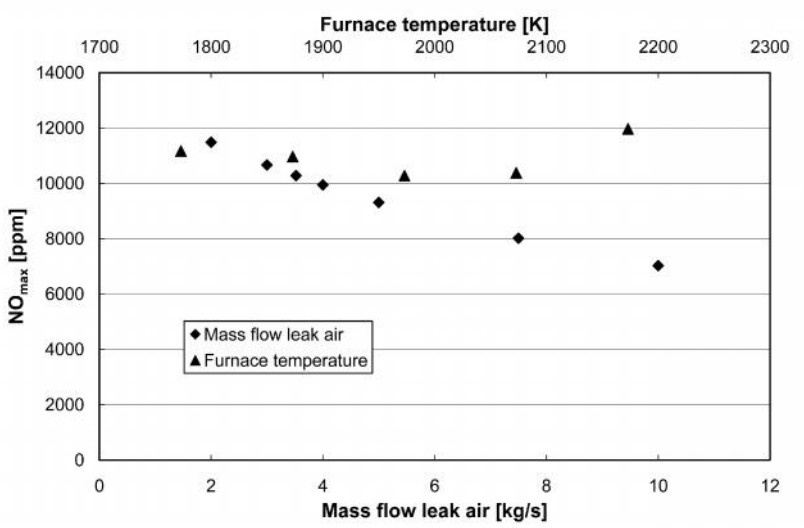

Figure 19: Influence of the temperature of the EAF freeboard reactor and of the air mass flow rate on the NO_{max} content in the furnace

The influence of the arc plasma reactor's parameters on NO_x concentration are depicted in Figure 20. An increase of the reactor volume leads to a higher NO_{max} content in the EAF freeboard, because of the longer retention time of the gas in plasma state. An increase of the temperature in the plasma reactor as well as an increase of the mass flow through it also leads to higher NO_{max} concentrations in the EAF freeboard. Therefore an increased power supply

by an increase of arc volume and plasma mass flow theoretically leads to increased NO_x formation in the arc.

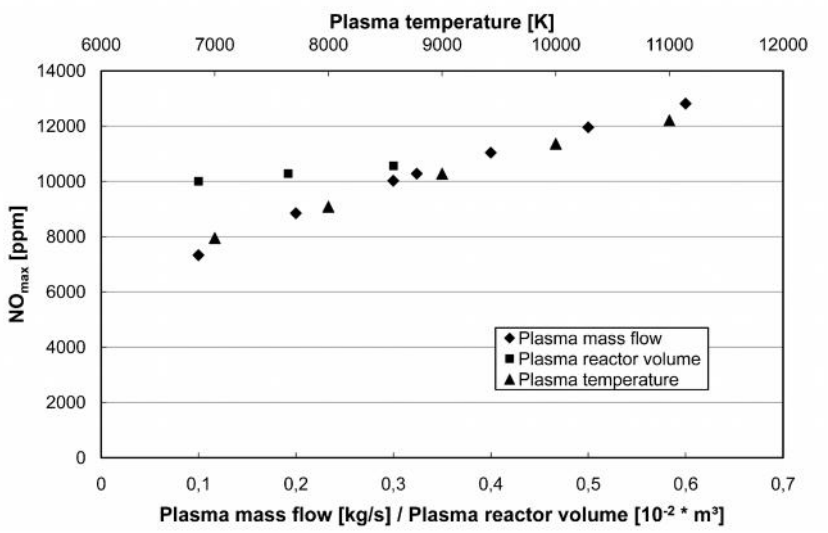

Figure 20: Influence of the arc plasma reactor parameters (volume, temperature, mass flow rate) on the NO_{max} concentration in the EAF freeboard reactor

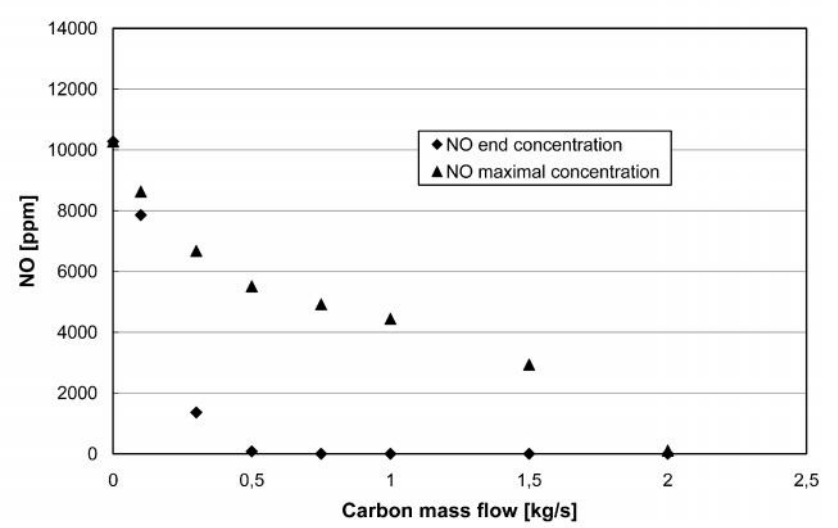

Figure 21: Influence of the rate of carbon addition on the NO_{max} and NO_{end} concentration in the EAF freeboard reactor

Finally the amount of carbon addition to the furnace was varied. As previously described the amount of carbon addition corresponding to electrode consumption is about 0.08-0.12 kg/s. A carbon addition of 0.5 kg/s represents a heat average for stainless steel production. During the slag foaming phase of a carbon steel grade a carbon mass flow of up to 2 kg/s was measured in the off-gas. Figure 21 shows the effect of different amounts of carbon addition on the NO content in the furnace. In this case the results were especially interpreted with respect to the maximum content NO_{max}, which appears in the form of a peak, and the steady end content

NO_{end}, which is reached after a certain time has elapsed during the simulation. As expected both values decline with rising carbon addition. However, the results show a different development of NO_{max} and NO_{end} with respect to the carbon mass flow rate. Whereas NO_{end} is already in the low ppm range for a carbon addition of 0.5 kg/s, the graph of the NO_{max} values at first shows an inflection point at about 1 kg/s carbon addition, for this carbon addition NO_{max} equals 4,500 ppm, before the NO_{max} values also decline to the low ppm range. Therefore only when higher amounts of carbon in form of CO, CO_2 in the furnace atmosphere is present the formation of the NO_x peaks is prevented.

In conclusion, the modelling of the electric arc furnace as a reactor network is in principal able to describe various events and phenomena influencing the gas phase of the investigated industrial EAF, such as the effect of air infiltration as well as CO and CO_2 formation through slag foaming or decarburization. It would also be possible to extend the model to include the effects of post combustion O_2 injectors and burners. Because of the great importance of chemical reaction kinetics in an EAF typical phenomena such as the measured NO_x peaks can only be reproduced using a model such as the reactor network model. Thermodynamic equilibrium calculations alone are not able to reflect these effects. Even though there are a number of considerable simplifications in the reactor network model, such as the assumption of an ideally stirred reactor, constant temperatures etc., the calculated NO_x concentrations within an order of magnitude are in good agreement with measurement data. However the influence of heat transfer, fluid flow, turbulence and geometry, such as for example the covering of the arc in foaming slag, cannot be reproduced with this kind of model.

Further sensitivity analysis, a refinement of the model and the extension to fluid flow and concentration gradients within the EAF freeboard and arc plasma using computational fluid dynamics (CFD) would be the next logical steps which would certainly lead to more detailed simulation results.

VII. SUMMARY

The pilot furnace trials as well as the thermodynamic equilibrium and chemical reaction kinetics calculations presented in this publication confirm the high NO_x formation potential of the electric arc furnace. The pilot furnace trial results show that an influence of the electric parameters of the arc on the NO_x formation cannot be confirmed, since this influence is negated by other more dominant effects, mainly the influence of the composition of the furnace atmosphere.

On the other hand, regarding the furnace atmosphere the results of the pilot EAF trials illustrate existing correlations between the O_2 and CO content of the furnace atmosphere and the resulting NO_x concentrations measured.

The thermodynamic calculations show that in an equilibrium state only rather small amounts of NO (< 30 ppm) even at temperature of up to 1,700 K are stable. If reducing gas species such as CO or H_2 are present, the equilibrium concentration of NO is even lower. A comparison of these results with measurements leads to the conclusion, that the off-gas of an EAF is usually not in thermodynamic equilibrium and that other factors such as chemical kinetics, an inhomogeneous concentration distribution, mass transfer etc. have a considerable influence on the NO concentration in the EAF's off-gas.

To take chemical kinetics into account, in a subsequent step the EAF was modelled as a reactor network. Calculations based on this model and data from an industrial electric arc furnace show that the model is principally able to describe phenomena such as the NO_x peak measured at ignition in the pilot EAF as well as industrial EAF's. Furthermore the calculated levels of NO concentration within an order of magnitude are in good agreement with measurement data.

The next logical step would be to extend the EAF modelling to incorporate fluid flow and concentration gradients within the EAF using CFD methods.

ACKNOWLEDGEMENT

The authors gratefully acknowledge the financial support from the European Community – Research Fund for Coal and Steel (RFSR-CT-2006-00033).

REFERENCES

1. J. C. Agarwal and N. S. Jessiman: Iron Steelmaker, 1992, vol. 19, pp. 23-24

2. H. D. Goodfellow, E. J. Evenson, X. Li, P. C. Mathur, M. J. Thomson: Proc. of 58th Electric Furnace Conf., ISS, Warrendale, PA, 2000, pp. 117-126

3. E. Chan, M. Riley, M. J. Thomson, E. J. Evenson: ISIJ Int., 2004, vol. 44, pp. 429-438

4. D. L. Hixenbaugh: AISTech 2005 Conf. Proc., AIST, Charlotte, 2005, pp. 629-635

5. M. Kirschen, L. Voj, H. Pfeifer: Clean Technol. Environ. Policy, 2005, vol. 7, pp. 236-244

6. M. Kirschen, L. Voj, H. Pfeifer: AISTech 2005 Conf. Proc., AIST, Charlotte, 2005, pp. 585-595

7. Y. Zeldovich, G. Barenblatt, V. Librovich, G. Makhviladze: The mathematical theory of combustion and explosions, Plenum Publishing Corporation, New York, 1985

8. F. Joos: Technische Verbrennung, Springer Verlag, Berlin, 2006

9. G. P. Smith, D. M. Golden, M. Frenklach, N. W. Moriarty, B. Eiteneer, M. Goldenberg, C. T. Bowman, R. K. Hanson, S. Song, W. C. Gardiner Jr., V. V. Lissianski, Z. Quin: http://www.me.berkeley.edu/gri_mech

10. Cantera, An object-oriented software toolkit for chemical kinetics, thermodynamics and transport processes, http://code.google.com/p/cantera

11. Pfeifer, H.: Energietechnische Untersuchung der Plasmatechnik bei der Stahlerzeugung, Verlag Stahleisen, 1992